SECOND EUROPEAN CONFERENCE ON EARTHQUAKE ENGINEERING
AND SEISMOLOGY, ISTANBUL AUG. 25-29, 2014

NUMERICAL STUDY FOR THE ASSESSMENT OF THE SEISMIC RESPONSE OF EARTH-RETAINING GRAVITY WALLS

Manya DEYANOVA[1], Carlo G. LAI[23] and Mario MARTINELLI[4]

ABSTRACT

The essence of performance-based design of gravity earth-retaining walls (*GRW*) lies in the estimation of the residual displacements following a given seismic event. Predictions of the permanent horizontal displacements and tilting are needed for an efficient capacity design based on allowable damage and models for seismic risk assessment and loss estimation. By knowing the possible failure mechanisms of a pre-designed gravity wall, engineers would be able to adjust the structure's geometry so to favour sliding as a predominant failure mechanism, since this is theoretically characterized by an infinite ductility. Accomplishment of this task however can be quite complicated due to the presence of two interacting phenomena: the coupled sliding and tilting of the rigid-body motion of the wall on an inelastic base and the generation of failure surfaces in the soil backfill. A lot of research has been carried out during the last 50-60 years on the seismic response of gravity walls under very general conditions. However, the results from this large amount of work are far from being complete and are still characterized by a large number of uncertainties.

The aim of the present study is to provide new conceptual insight into the seismic response of monolithic gravity retaining walls. A large number of fully non-linear, time-history analyses of *GRW*s are performed using advanced numerical modelling. Different types of soil parameters and varying wall geometry within practical range are investigated. The influence of different ground motion parameters (*GMP*) is discussed and the results are compared with some of the most common limit equilibrium Newmark's sliding block procedures, including the recommendations of EN1998-5. Apart from its empirical nature, the research gives practical guidelines and recommendations for the displacement-based design of *GRW*s.

INTRODUCTION

Gravity retaining walls are the oldest and most common earth retaining structures, which can be explained with their easy and economical construction, inspection and retrofit. They fall into the category of externally stabilised, rigid, self-standing systems and nowadays are mostly built of monolithic reinforced concrete. Although their design for gravity loads is considered simple from engineering point of view, post-earthquake reconnaissance (Fang, et al., (2003), Zhang, et al., (2011)) and experiment tests (Anderson, et al., (1987), Cascone, et al., (1995), Simonelli, et al., (2000), Carafa, et al., (1998), Watanabe, et al., (2003), Lo Grasso, et al., (2004)) have shown that the prediction of their predominant failure mode and residual displacements under seismic action is still a

[1] PhD student, ROSE Programme, UME School, IUSS Pavia, Italy, Institute for Advanced Study - manya.deyanova@umeschool.it
[2] Assoc. Prof., Department of Civil Engineering and Architecture, University of Pavia, Italy - carlo.lai@unipv.it
[3] European Centre for Training and Research in Earthquake Engineering (EUCENTRE), Pavia, Italy
[4] Marie-Curie Research Fellow at Deltares, The Netherlands - mario.martinelli@deltares.nl

serious challenge for the present design methods. One of the main reasons is that the seismic response of *GRW* is a complex combination of the three failure modes: sliding, tilting and gross instability, bound together by the soil-structure interaction phenomenon occurring at the foundation level and behind the wall with the backfill. The displacement of the wall affects the distribution of the soil pressure in the backfill and the base, which in turn affects the displacement of the wall. With the outward movement of the wall, the active soil wedge slides downwards along the failure surface, causing settlement and tension cracks in the backfill. And if the bearing capacity of the soil under the toe of the wall is not sufficient, the wall tilts and may even overturn. Fig. 1 presents possible wall failures of the wall-backfill system.

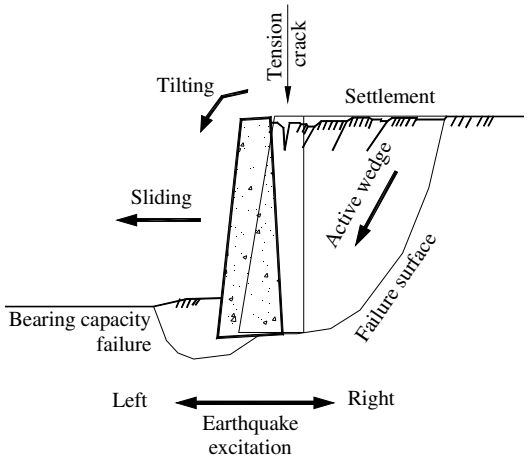

Figure 1. Combined failure modes for wall-backfill system

Lot of analytical research on the seismic response of *GRW* has been done in the last 50-60 years and many analytical methods for the evaluation of the residual displacement have been proposed. The most widely used (listed in Table 1) are different modifications of the pseudo-dynamic Newmark sliding block procedure. The latter is a limit equilibrium analysis method, based on the concept of allowable displacements and Mononobe-Okabe (*M-O*) active soil wedge. The assumptions for all the listed methods are that 1) the failure surfaces are predefined and rectilinear, 2) constant strength develops along these surfaces and 3) failure occurs as a combination of wall sliding and rigid body motion of the soil wedge. No wall tilting and no deformability of and interaction with the adjacent soil are taken into account. What is more, all the methods require an educated guess for the point of application of the soil thrust (usually taken at 0.5*H*) and a value for the yielding acceleration a_y, which is either assumed (*0.4 -0.6)PGA,* or is based on static equilibrium in sliding with *M-O* soil wedge.

Table 1. Simplified Newmark's block-on-plane models for calculating earthquake induced displacements

Reference	Model	Reference	Model
(Newmark, 1965)	$d_{perm.} = \frac{v_{max}^2}{2a_y}\frac{a_{max}}{a_y} \quad \frac{a_y}{a_{max}} > 0.17$ upper bound modified later on to $d_{perm.} = \frac{v_{max}^2}{2a_y}\left(1 - \frac{a_y}{a_{max}}\right)\left(\frac{a_y}{a_{max}}\right)^{-2}$	(Zarrabi, 1979)	$d_{perm} = R_v R_z \frac{37 v_{max}^2}{a_{max}} exp\left(\frac{-9.4 a_y}{a_{max}}\right)$ $R_v = 1.015 - 0.2\frac{a_y}{a_{max}} + 0.72\left(\frac{a_y}{a_{max}}\right)^2$ $R_z = 0.7 + 1.2a_y(1 - a_y) \quad a_y < 0.3$
		(Nadim, et al., 1983)	$d_{perm} = \frac{v_{max}^2}{a_{max}} exp\left(9.4\left(0.66 - \frac{a_y}{a_{max}}\right)\right)$ 95% confidence that $d_{perm.}$ is not exceeded
(Sarma, 1975)	$d_{perm,5\%\,PE} = \frac{\alpha \cdot a_{max} T^2}{4} 10^{\left(1 - 3.86\frac{a_y}{a_{max}}\right)}$ 5%PE – 5% probability of eccedance	(Whitman, et al., 1985)	$d_{perm} = \frac{37 v_{max}^2}{a_{max}} exp\left(\frac{-9.4 a_y}{a_{max}}\right)$ mean fit
(Richard, et al., 1979)	$d_{perm} = \frac{0.087 v_{max}^2 a_{max}^3}{a_y^4}$ upper bound	(Cai, et al., 1995)	$d_{perm} = \frac{35 v_{max}^2}{a_{max}} exp\left(\frac{-6.91 a_y}{a_{max}}\right)\left(\frac{a_y}{a_{max}}\right)^{-0.38}$ mean upper bound

Table 1 also demonstrates the choice by the different researcher on the most influential *GMP* for the estimation of the horizontal residual displacement. The formulae use peak ground acceleration (*PGA*), peak ground velocity (*PGV*) and predominant period (*T*) as detrimental for d_{perm}. Other researchers, however, consider Arias intensity (I_a) and Dobry duration (*DD*) as critical. For example, Smith, (1994) analysed the Newmark displacements for six values of critical acceleration under 227 digitalised strong-motion records and demonstrated a pattern between d_{perm} and I_a. Jibson, (1993) performed a similar research and proposed a relationship between d_{perm}, I_a and a_y. Garini, et al., (2011), on the contrary, came to the conclusion that I_a cannot alone be a reliable predictor for sliding, especially with motions containing acceleration pulses of long duration. However, all the aforementioned studies dealt with the ideal Newmark sliding model, in which the only non-linearity is represented by the Coulomb friction at the base.

The Newmark block-on-plane concept forms also the bases of different design code provisions. For example, Chapter 7 of Eurocode 8, Part 5 (EN1998-5:1994, 2004) begins by setting very high requirements for the analysis of an earth retaining structure. According to them phenomena like the non-linear soil response while in dynamic interaction with the structure and compatibility between the soil and wall deformations should be taken into account. Yet, the model proposed by the code is based on the limit-equilibrium pseudo-dynamic approach with *M-O* active soil wedge and horizontal and vertical acceleration. In this model the most debated parameter is factor *r* for the calculation of the horizontal seismic coefficient $k_h=(a_{gR}\cdot\gamma_I\cdot S)/(g\cdot r)$. On one hand, the code gives large values for k_h resulting in a very few cases of gravity retaining walls meeting the stability requirement for sliding. On the other hand, several aspects are not explicitly mentioned, such as: the value of this reduction coefficient for structures that could accept greater displacements than those listed in Table 2, Chapter 7.3.2.2 of EN1998-5:1994, (2004); or the amount of residual displacement for systems with safety factor for sliding greater than 1.

For the present study definition of the horizontal wall displacement at failure is mandatory. It depends on the functionality of the wall and the expected level of damage for the supported structure. However, it is also directly related to the mobilisation of soil strength in the backfill with the corresponding soil strength degradation. Huang, et al., (2009) addressed the latter issue by performing a series of shaking table tests. He proposed a range of admissible horizontal wall displacements according to the mobilized friction angle along the shear band in the backfill. The tests showed that the friction angle starts to deteriorate from φ_{peak} to $\varphi_{\text{operational}}$ at displacement levels of *d/H*=2.9-3.2% and after displacements of *d/H*=3.4-4.1% the critical state condition was attained. Based on that and the assumptions for the development of a single shear band in the backfill, the authors proposed the conservative value for displacement at failure of *d/H*=5%. Wu, et al., (1996) on the contrary recommended 10% of *H* as a wall failure horizontal displacement. These and other displacement criteria are compared in Table 2. In the present numerical study 10%·*H* is adopted.

Table 2. Comparison of permissible displacements for *GRW*s

	(EN1998-5:1994, 2004) [1]	**(AASHTO, 2002)**[2]	**(Wu, et al., 1996)**	**(Huang, et al., 2009)**	**(JRTRI, 1999)**
Permissible horiz. displ.	$d_r = 300\alpha S$ $d_r = 200\alpha S$ $\alpha = \frac{\gamma_I \alpha_{gR}}{g}$	$d_r = 250\alpha$ $\alpha -$ design ground acc.	2%·*H*	2%·*H*	
Failure horiz. displ.			10%·*H*	5%·*H*	
Permissible settlement					0.1-0.2m [3] Damage Level 3
Severe settlement					>0.2m [4] Damage Level 4

[1] An upper boundary for the range of validity of factor *r*. It is not explicitly said whether the limitations are for SLS or ULS.
[2] Refers to abutments and when minimum damage is required at the abutment support.
[3] When minor retrofit for the abutments is required.
[4] When long-term retrofit of the abutments could be accepted.

PARAMETRIC STUDY

Seventeen sets of ten non-linear time history analyses are performed with the explicit, finite difference program FLAC2D (Itasca Consulting Group). Each analysis has its own unique name that gives the basic information of the case it represents, as shown on the scheme below:

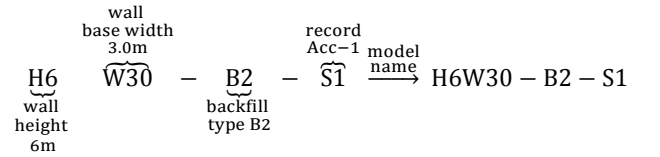

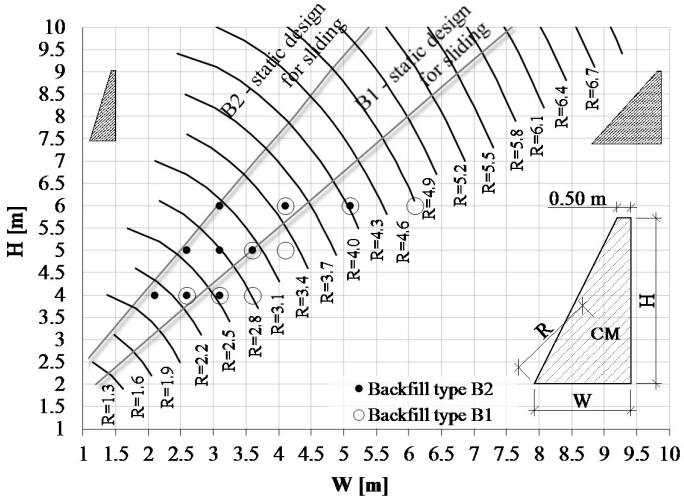

Figure 2. Wall geometries considered in the analyses

Wall Geometry

The walls are trapeziums with fixed top width of 0.5m and varying height and base width. Fig. 2 shows the wall geometries for the two types of backfill: loose sand (B1) with black dots and dense sand (B2) with circles. First, the wall geometry is selected within the range of practical cases. Second, only these cases that satisfy the requirements for static design according to EN1997-1, (2004) are chosen. The static design is governed by the sliding capacity for GEO Limit Sate, Approach 1 with $\gamma_{R,h}=1$ or Approach 2 with $\gamma_{R,h}=1.1$ according to EN1997-1, (2004), Chapter 2.4.7. The wall geometries onto the lines have over deign factor $ODF=\gamma_{R,h}$ and those below the lines (each corresponding to the indicated backfill type) lead to a greater partial safety factor.

Soil Types and Constitutive Models

Two soil types for the backfill are considered: loose sand (B1) and dense sand (B2). The foundation soil, the layer immediately under the wall, is soil type B2. The main layers are divided into sub-layers (see Fig. 3) each assigned soil properties according to its average mean effective stress, as shown in Table 3. The soil is modelled as a non-linear continuum with shear stiffness degradation rule according to Darendeli, (2001) associated with Mohr-Coulomb failure criterion. The base layer (the bedrock) and the wall are modelled as linear-elastic materials.

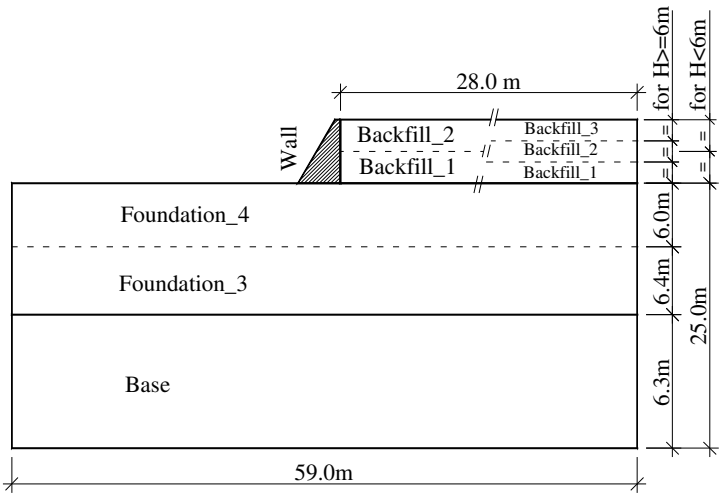

Figure 3. Sketch of the soil layers and sub-layers used in the models

Table 3. Soil properties used in the analyses

Layer	Soil type	e [1]	ρ [kg/m^3]	φ [°] [2]	K_0	G_0 [3] [Pa]	K	c	ψ [°]	Model
Backfill	B1	0.65	1700	27.5	1-sinφ	$7000\frac{(2.17-e)^2}{1+e}(\sigma'_0)$	2.16G_0	0	5	Non-linear hysteretic + Mohr-Coulomb failure criterion + viscos damping
	or									
	B2	0.45	2000	37.5						
Foundation	B2	0.45	2000	37.5						
Base	Bed rock	-	2400	-		2e9	2.0G_0	-		Linear visco-elastic
Wall	-		2400			2.2e9	3e9			
[1] (Bowles, 1984)			[2] (Kulhawy, et al., 1990)							[3] (Ishihara, 1996)

Selection of records

Ten real accelerograms from outcropping rock sites are selected and scaled to satisfy the criterion for spectrum compatibility. The target response spectrum is Type 1 on Soil A according to EN1998-1, (2004) with *PGA*=0.28g. The records are scaled so that the difference of the average and the target spectra is less than 10% in the period range 0.15-2.0s. The events and the *GMP*s of the records after scaling are listed in Table 4. It is evident that *PGA*, as an indirect selection criterion, varies in a small range, whereas the other *GMP*s show a much greater dispersion.

Table 4. Records used in the analyses

Original							Scaled					
Record	**Earthquake**	**Site**	**Fault**	**M_w**	**Epic. distance**	**PGA [m/s^2]**	**Scaling factor**	**PGA [m/s^2]**	**PGV [m/s]**	**I_a [m/s]**	**T [s]**	**DD [s]**
Acc_1	Izmit,1999	rock	strike-slip	7.6	113 km	2.46	1.03	2.53	0.24	1.02	0.42	36.2
Acc_2	Umbria Marche,1997	rock	normal	6	38.0 km	0.97	3.35	3.26	0.50	2.61	0.18	30.0
Acc_3	Tabas,1978	rock	oblique	7.3	12.0 km	3.48	1.16	4.04	0.21	2.14	0.16	32.4
Acc_4	Montenegro,1979	rock	thrust	6.9	65.0 km	2.30	1.27	2.92	0.17	1.19	0.26	10.9
Acc_5	Campano Lucano,1980	rock	normal	6.9	80.0 km	0.64	3.25	2.07	0.18	1.06	0.66	31.7
Acc_6	Loma Prieta,1989	rock	reverse-oblique	6.9	28.6 km	5.00	0.35	1.75	0.14	0.21	0.38	3.45
Acc_7	Eastern Honshu,2003	rock	uknown	7	50.5 km	1.65	2.44	4.03	0.37	4.24	0.10	27.6
Acc_8	Kyushu,2005	rock	uknown	6.6	36.2 km	1.38	2.81	3.87	0.33	1.67	0.08	13.0
Acc_9	Eastern Honshu,2008	rock	uknown	6.9	23.1 km	2.24	1.16	2.60	0.26	1.74	0.36	19.9
Acc_10	Eastern Honshu,2008	rock	uknown	6.8	99.3 km	3.72	0.74	2.75	0.11	0.33	0.42	10.4
							mean	2.98	0.25	1.62	0.30	21.6
							coefficient of variation δ	0.27	0.48	0.73	0.60	0.53

DESCRIPTION OF THE NUMERICAL MODEL

The soil layers and the wall geometries described above are modelled with the finite difference 2D plain-strain code FLAC 7.0. The continuum is divided into square zones of size smaller than 1/8 to 1/10 of the wavelength associated with the highest frequency component that contains appreciable energy. This is to avoid inaccuracies in modelling the deformation field. The analysis is performed in three stages: 1) Static equilibrium due to the self-weight of the base layers only; 2) Static equilibrium when the weight of the backfill layers and the wall are activated; 3) Dynamic time-history analysis of the whole system. The boundaries are set at a considerable distance away from the wall to avoid near-filed effects and are set as fixed for the first two stages of static analysis; then they are replaced by quite (viscous) and free-field boundaries for the dynamic solution. A view of the mesh is shown in Fig. 4.

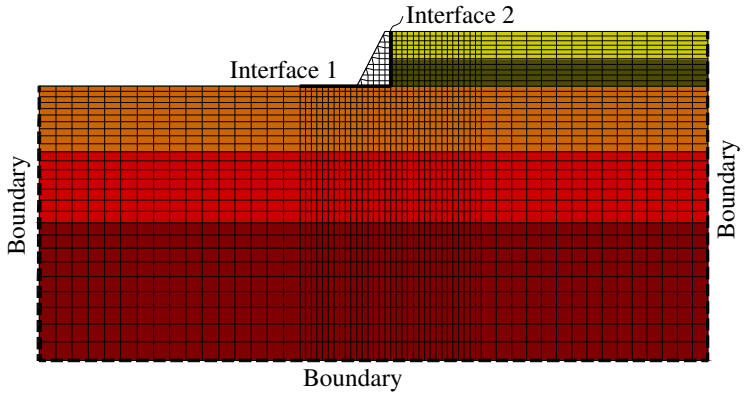

Figure 4. View of the mesh. Different colours represent different soil sub-layers

Damping is introduced in the models through three different mechanisms. In the small strain range stiffness proportional viscous damping is used. It also improves the convergence and removes high frequency noise. In the intermediate strain range (i.e. for moderate strains) the shear modulus degradation curves (G/G_{max}) combined with the Masing rule provides hysteretic damping. Finally, when the mobilized stress touches the yield surface, the Mohr-Coulomb failure criterion provides another source of energy dissipation, which is due to the soil plastic response.

The contact surfaces between the wall and the surrounding soil are modelled with interface elements (see Fig. 4). They are characterised by Coulomb friction angle of 0.6φ and $2/3\varphi$ for Interface 2 and Interface 1 respectively and by no cohesion. They also have normal and shear stiffness but no tensile and shear bond strength. The exact values of the stiffnesses are not important, as long as they are large enough to prevent relative movement at the interfaces before failure and at the same time low enough to keep the speed of the convergence higher. The behaviour of these interface elements has been tested under dynamic loading through a simple FLAC model of a rigid block on a linear-elastic half-space subjected to a Ricker-wavelet signal. The residual horizontal displacements have been compared with the analytical solution and with the solution obtained by the Java program by Randall Jibson and Matthew Jibs called Newmark, available on the USGS web-site. The comparison showed very good agreement with the FLAC interface elements under dynamic excitation.

RESULTS

Analysis of the results

The failure patterns observed in the FLAC models clearly show that the formation of a failure surface in the backfill is coupled with significant deformation of the soil under the toe of the wall and with soil settlement behind the wall. This is quite evident in Fig. 5, in which the horizontal displacement contours of one of the case-studies (H6W30-B2-S1) are presented. For the same case the relative

horizontal displacement of the wall base (D), the tilting ($tan\Theta$) and the settlement of the soil surface behind the wall (w) are shown in Fig. 6. D is obtained by subtracting from the horizontal wall movement the free field displacement recorded at the top of the foundation layer away from the wall and is negative when the wall base moves away from the backfill. $tan\Theta$ is computed as the ratio between the difference in the vertical displacements of the two ends of the base of the wall and the base width W and is negative if the wall rotates anticlockwise. Lastly, the vertical displacement of the soil surface behind the wall is negative, when it denotes settlement. An interesting observation is that this settlement spreads away from the wall at a distance greater than the wall height, as Fig. 6 shows.

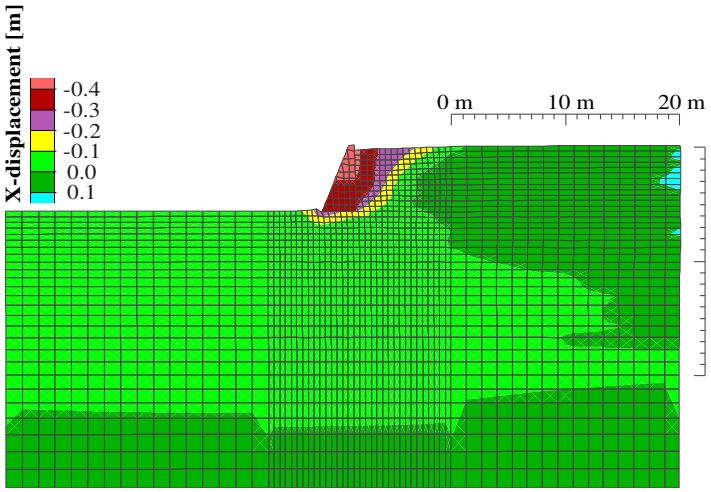

Figure 5. Horizontal displacement contours at the last step of the dynamic solution for the case H6W30-B2-S1

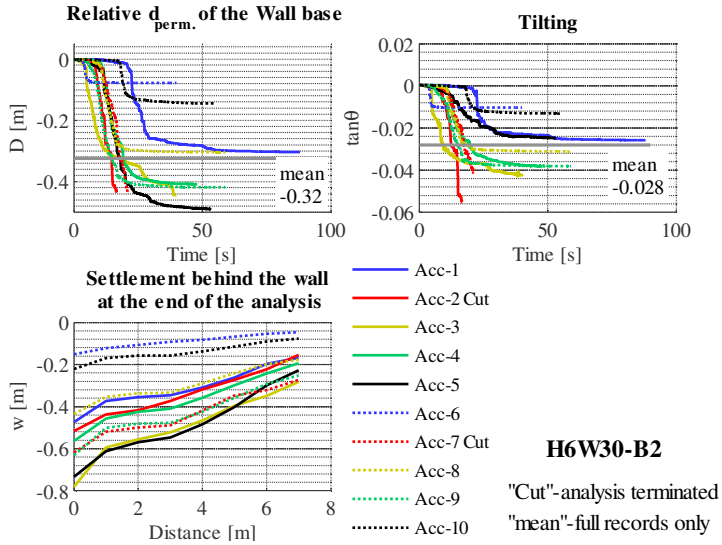

Figure 6. Results from the FLAC analysis for case H6W30-B2-S(1-10)

Two types of failure mechanisms are distinguished. The first one is due to large deformations at the soil base and the second one is due to residual wall horizontal displacements greater than $0.1 \cdot H$. For the first type, the analyses could not be performed until the end of the records because of these excessive deformations in the foundation soil and these cases are denoted in Fig. 6 with "Cut" after the record. The mean values are presented with a horizontal grey line but they include only the non-failing records. It is worth noting that the residual horizontal displacements and tilting obtained from one set of records fall into a very wide scatter, which casts doubts on the applicability of the mean value for the prediction of the final wall displacement.

Table 5 summarises the results from the analyses for all the cases. The first two columns denote the number of cases within a set that fail due to one of the accepted failure modes. For all the cases this happens under records Acc_2 and Acc_7, which are the records with the highest Arias Intensity. This question will be addressed in details later on. The next four columns show the mean values of the permanent horizontal displacement and tilting and the corresponding coefficient of variation (δ).

Table 5. Summary of the results from FLAC models

Case	Number of failing cases within a SET		$d_{perm.}$ [1]		tan(Θ) [1]		Case	Number of failing cases within a SET		$d_{perm.}$ [1]		tan(Θ) [1]	
	Low bearing capacity at the base	$d_{perm.}$> 0.1H	μ [2] [m]	δ	|μ| [3]	δ		Low bearing capacity at the base	$d_{perm.}$> 0.1H	μ [2] [m]	δ	|μ| [3]	δ
H6W50-B2	-	-	-0.15	0.62	0.0036	0.64	H6W60-B1	-	-	-0.19	0.45	0.0024	0.88
H6W40-B2	-	-	-0.26	0.59	0.0099	0.75	H6W50-B1	-	-	-0.25	0.50	0.0066	0.68
H6W30-B2	2	-	-0.32	0.46	0.0280	0.42	H6W40-B1	2	-	-0.27	0.42	0.0017	0.97
H5W35-B2	-	-	-0.19	0.61	0.0037	0.56	H5W40-B1	-	-	-0.26	0.49	0.0056	0.87
H5W30-B2	-	-	-0.27	0.49	0.0152	0.46	H5W35-B1	-	2	-0.33	0.48	0.0134	0.55
H5W25-B2	2	-	-0.27	0.42	0.0290	0.41	H4W35-B1	-	-	-0.16	0.12	0.0049	0.95
H4W30-B2	-	-	-0.12	0.58	0.0040	1.00	H4W30-B1	-	-	-0.22	0.45	0.0065	0.67
H4W25-B2	-	-	-0.18	0.52	0.0074	0.64	H4W25-B1	-	2	-0.29	0.42	0.0149	0.78
H4W20-B2	-	2	-0.25	0.045	0.0275	0.88							

[1] The mean valuse are calculated only with the "non-failing" cases
[2] The negative values denote displacement away from the backfill
[3] The maen of the absolute values

Comparison with the design methodology by EN1997-1 and EN1998-5

The "failing" cases are marked in Fig. 7. The grey dots and the grey circles mark the "failing" walls with backfill type B2 and B1 respectively. The exact values of *ODF* for sliding according to EN1997-1, (2004) are compared with the mean horizontal wall displacements from the FLAC models (d_{FLAC}^{mean}) in Table 6. The results lead to the conclusion that if a wall is designed with *ODF* for sliding greater than 1.35 and 1.2 (partial factors considered according to EN1997-1, (2004)) for backfill of dense and loose sand respectively, the wall is unlikely to fail in regions of medium to high seismicity with *PGA* between 0.2g and 0.35g. However, there is no proportionality between the *ODF* and the expected seismic residual horizontal displacement. For example, case H6W60-B1 has a larger mean horizontal displacement than case H4W35-B1 but at the same time its *ODF* for static design is also larger. In the similar manner, case H6W40-B2 responds with much larger residual displacement than case H4W25-B2 but they both have the same *ODF*.

The last three columns of Table 6 compare the displacements from the numerical models with those obtained from the seismic design procedure according to EN1998-5. The assumption is that if the allowable displacement for certain factor *r* corresponds to a sliding condition coefficient *E/R=1*, for greater values of this ratio the final displacement should be proportional to it. The design parameters are the following:

- Importance factor $\gamma_I=1$
- Soil factor $S=1.15$ for soil Type C
- Response spectrum Type 1 with $a_{gR}=0.28g$
- Horizontal seismic coefficient calculated $k_h=0.161$
- Vertical seismic coefficient assumed $k_v=0$
- Factor $r=2$ and corresponding allowable displacement $d_r=0.097m$
- Final residual displacement assumed $d_{perm.} = d_r \cdot \frac{Total\ horizontal\ design\ force\ (E)}{Resisting\ against\ sliding\ force\ (R)}$

The comparison shows that under the above stated assumptions the EN1998-5 procedure tends to underestimate the horizontal residual displacements of *GRW*.

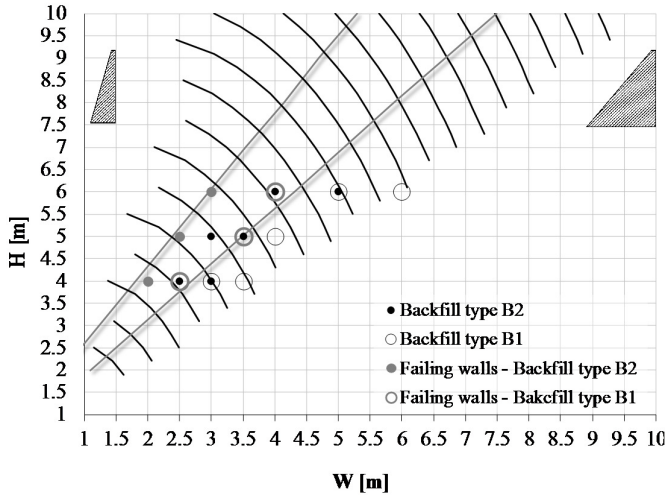

Figure 7. "Failing" walls from the FLAC models, plotted against the range of static design for sliding according to EN1997-1

Table 6. Comparison between the $d_{perm.}$ from the FLAC models and the Eurocode design procedures

W [m]	H [m]	d_{FLAC}^{mean} [m]	EN1997–1	EN1998-5		
			ODF sliding	d_r [m]	E/R	d_r*E/R
Backfill type B2						
5	6	0.15	1.67	0.097	1.33	0.13
4	6	0.26	1.39		1.49	0.14
3	6	fail	1.11		1.74	0.17
3.5	5	0.19	1.47		1.44	0.14
3	5	0.27	1.31		1.56	0.15
2.5	5	fail	1.14		1.71	0.17
3	4	0.12	1.60		1.36	0.13
2.5	4	0.18	1.39		1.49	0.14
2	4	fail	1.18		1.67	0.16
Backfill type B1						
6	6	0.19	1.46	0.097	1.38	0.13
5	6	0.25	1.25		1.52	0.15
4	6	fail	1.04		1.73	0.17
4	5	0.26	1.22		1.54	0.15
3.5	5	fail	1.10		1.66	0.16
3.5	4	0.16	1.35		1.44	0.14
3	4	0.22	1.19		1.57	0.15
2	4	fail	1.04		1.73	0.17

Comparison with simplified Newmark's block-on-plane models

Due to the uncertainties related to the value of the yielding acceleration a_y needed for the Newmark procedures in Table 1, the comparison is performed not case-by-case but via intersecting areas of applicability. The calculations with the Newmark's models are performed with the *PGAs*, *PGVs* and *Ts* for each record. The a_y is calculated through an iterative process for finding force equilibrium with *M-O* soil wedge, following an example by Kramer, (1996). The exact values are listed in Table 7.

Table 7. Yielding acceleration for each case considering equilibrium with M-O soil wedge

Case	H6W50-B2	H6W40-B2	H6W30-B2	H5W35-B2	H5W30-B2	H5W25-B2	H4W30-B2	H4W25-B2	H4W20-B2
a_y [m/s^2]	2.37	2.11	1.74	2.195	2.01	1.78	2.31	2.11	1.84
Case	H6W60-B1	H6W50-B1	H6W40-B1	H5W40-B1	H5W35-B1	H4W35-B1	H4W30-B1	H4W25-B1	
a_y [m/s^2]	2.065	1.815	1.49	1.79	1.60	1.95	1.74	1.49	

The horizontal displacements, obtained from the methods in Table 1 with a_y from Table 7 are plotted in Fig. 8 with respect to a_y/PGA. The values of $d_{perm.}$ are calculated among all cases. The area enclosed by the maximum and minimum displacements for each simplified method is shaded in grey. The darkest area corresponds to the range of validity of all the methods plotted. The vertical line shows the minimum a_y/PGA among all the cases for one type of backfill. In other words, the horizontal displacements obtained from the simplified methods belong to the shaded area to the right of the vertical line. The horizontal lines correspond to the maximum and minimum horizontal displacements from the FLAC models among all cases for each backfill type. Thus, the intersection between the hatched and the shaded areas shows the range of a_y/PGA, where the Newmark's methods give horizontal displacements close to those obtained with the numerical models. Apparently, the residual horizontal wall displacements calculated through the Newmark procedures with the yielding acceleration based on the *M-O* active wedge assumption could be significantly underestimated and the predictions are more reliable with $a_y < 40\%PGA$. The method by Nadim, et al., (1983) for high values of *PGA* leads to results most close to those from the FLAC models.

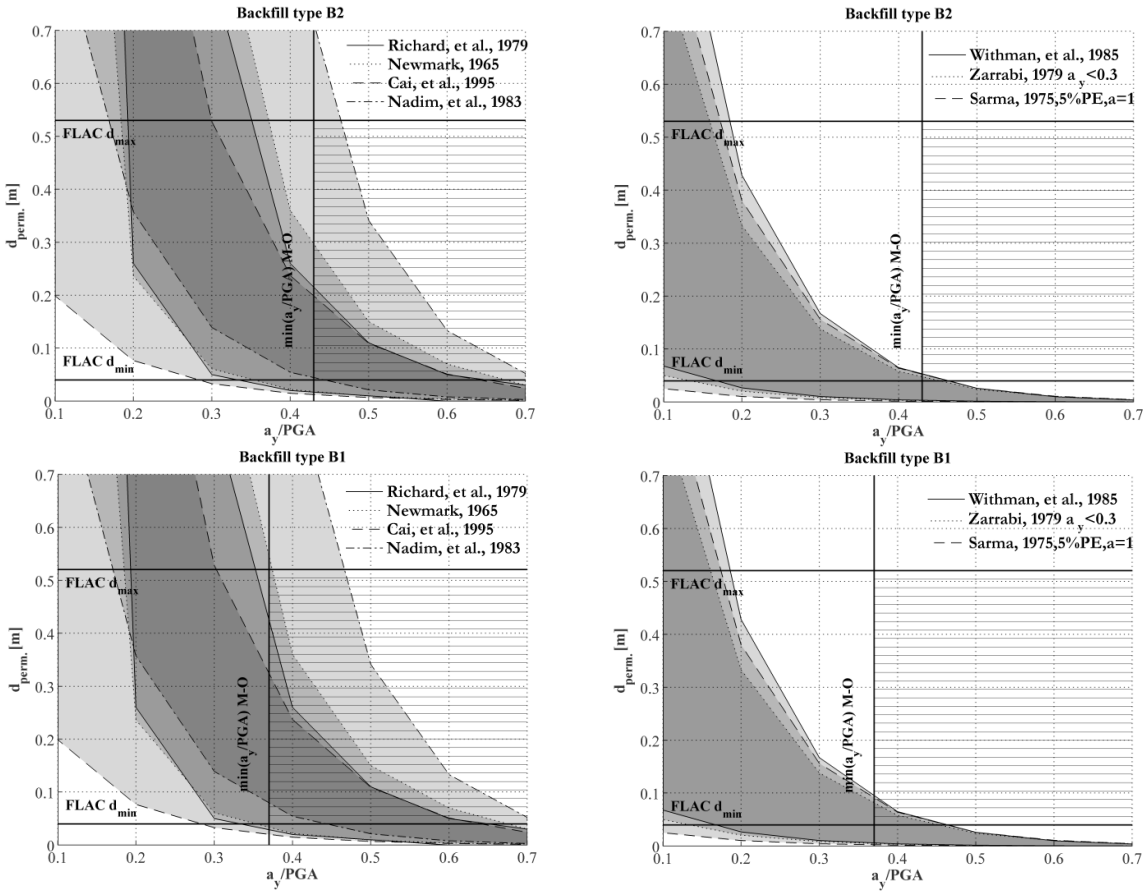

Figure 8. Comparison between 7 Newmark's methods and results from 170 FLAC models

The influence of GMPs on the residual horizontal wall displacement

As already mentioned, $d_{perm.}$ from the FLAC analyses shows wide dispersion within the set of spectrum compatible records (see Fig. 6). This implies that the mean value is not a reliable parameter for the prediction of the final permanent displacements. Using the maximum displacement within a case study is also not justifiable because it could lead to significant overestimation. Having in mind that the record selection is indirectly related to *PGA*, together with the conclusions from Fig. 8, a logical question arises about the influence of different *GMP*s. In Fig. 9 $d_{perm.}$ of the cases with H=6m and backfill type B2 are plotted against *PGA*, *PGV* and I_a. The models that fail due to excessive deformation of the base soil are excluded. The graph shows clearly that a relationship between the horizontal displacements and *PGA* could hardly be established but a very evident pattern exists with the Arias Intensity.

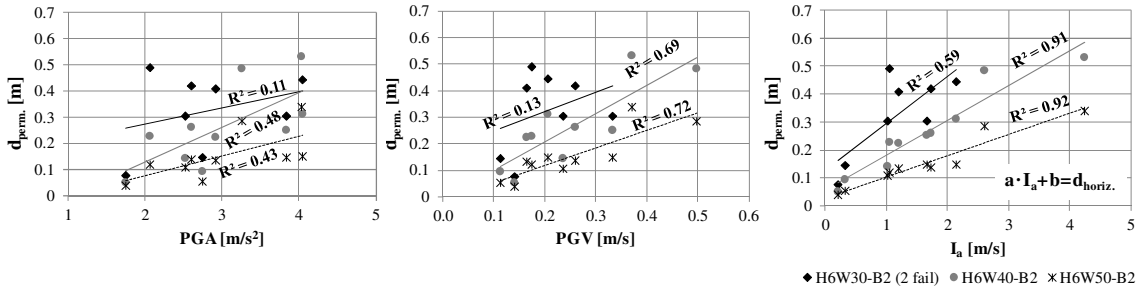

Figure 9. Relationship between *GMP*s and $d_{perm.}$ for the cases with H=6m and backfill B2

The same trend has been found for all other cases. This leads to the conclusion that a relationship between $d_{perm.}$ and I_a, together with parameters related to the wall geometry and soil type can be developed to serve the purpose of a predictive equation and a vulnerability function. It has to be combined, however, with an appropriate attenuation relationship for I_a, as the code provisions do not give any recommendations for the seismic hazard expressed in terms of Arias Intensity.

CONCLUSIONS

In the present study 17 sets of 10 fully non-linear time-history analyses of *GRW*s with different geometry are performed. Two types of backfill are considered: loose and dense sand and only dense sand for the base soil. The performance of the models is tested and validated. The results are analysed and compared with well-known procedures for design of gravity retaining walls. The following conclusions are reached:

- A *GRW* behaves under seismic action as an integrated system of three parts – the rigid wall, the non-linear soil wedge and the foundation soil. Good understanding of the deformability and capacity of these three components, the interaction among them, how different ground motion parameter influence them and how to quantitatively distinguish different failure modes, is the key to displacement-based design of gravity retaining walls;
- The settlement in the backfill spreads away from the wall at a length greater than the wall height;
- The residual horizontal displacements from a set of 10 spectrum compatible records vary significantly;
- The following design recommendations are given: for the cases within the frame of the present study if the wall with backfill of dense sand is designed with over-design factor (*ODF*) for sliding greater than 1.35 and for the backfill of loose sand with *ODF*>1.2 ((EN1997-1, 2004) all partial factors considered), the wall is unlikely to fail in regions of medium-high seismicity with *PGA* between 0.2 and 0.35g, where failure is considered either loss of bearing capacity under the toe of the wall or residual horizontal displacements greater than 10% of the height of the wall;
- Under the stated assumptions, the Eurocode 8, Part 5 procedure tends to underestimate the residual displacements of *GRW*s under seismic action;
- A comparison between the numerical models and some Newmark's block-on-plane methods shows that when a_y is calculated from static equilibrium with M-O soil wedge, the latter methods underestimate the residual horizontal wall displacement;
- Relationship between $d_{perm.}$ and *PGA* cannot be established but a very evident pattern exists with I_a, which can be expressed in a predictive equation for the wall residual horizontal displacement as a function of H, W, type of backfill and I_a.

ACKNOWLEDGMENTS

The work presented in this paper was partially supported by the financial contribution of the Italian Department of Civil Protection within the framework "RELUIS-DPC 2010-2013 (*Linea AT2.1 – Macro-Tema MT3 - Opere di sostegno rigide e flessibili*)". This support is greatly acknowledged by the authors.

ACRONYMS AND SYMBOLS

DD	*D*obry *D*uration	γ_I	importance factor (see EN 1997-1)
GMP	*G*round *M*otion *P*arameter	$\gamma_{R,h}$	partial factor for sliding and bearing resistance
GRW	*G*ravity *R*etaining *W*all		(see EN 1997-1)
M-O	Mononobe – Okabe	μ	mean value
ODF	*O*ver-*D*esign *F*actor (see EN 1997-1)	ρ	bulk mass density
PE	*P*robability of *E*xceedance	σ'_0	mean effective stress
PGA	*P*eak *G*round *A*cceleration	σ	standard deviation
PGV	*P*eak *G*round *V*elocity	φ	angle of internal friction
SLS	*S*erviceability *L*imit *S*tate	ψ	dilation angle
ULS	*U*ltimate *L*imit *S*tate		
		k_h	horizontal seismic coefficient
a_{gR}	reference peak ground acceleration on type A soil	k_v	vertical seismic coefficient
a_{max}	peak ground acceleration	K	bulk modulus
a_y	critical/yielding acceleration	K_o	coefficient for lateral earth pressure
c	cohesion	M_w	moment magnitude
d	horizontal wall displacement	r	reduction coefficient (see EN 1998-5)
$d_{perm.}$	residual horizontal displacement of the wall	R	resisting force against sliding
d_r	allowable horizontal displacement (see EN 1998-5)	S	soil factor (see EN 1998-1)
D	horizontal displacement of the wall base	$tan(\Theta)$	tilting of the wall
e	void ratio	T	predominant period at which the maximum
E	total horizontal design force		spectral acceleration at 5% damping occurs
G_0	initial shear modulus	v_{max}	peak ground velocity
H	wall height	w	settlement behind the wall
I_a	Arias intensity	W	width of the wall base

REFERENCES

AASHTO Standard specifications for highway bridges [Book]. - Washington, D.C. : American Association of State Highway and Transportation Officials, 2002. - Vol. Secs. 3 and 7.

Anderson GR, Whitman RV and Germaine JT Tilting response of centrifuge-modeled gravity retaining wall to seismic shaking [Report]. - Cambridge, MA : Department of Civil Engineering, Massachusetts Institute of technology, 1987.

Bowles Joseph E. Physical and Geotechnical Properties of Soil [Book]. - [s.l.] : Halliday Lithograph Corporation, 1984.

Cai Z. and Bathurst R. J. Deterministic sliding block methods for estimating seismic displacements of earth structures [Journal] // Soil Dynamics and Erathquake Enginnering 15. - 1995. - pp. 255 - 268.

Campbell K. W. and Duke C. M. Bedrock intensity, attenuation, and site factors from San Fernando earthquake records [Journal] // Bulletin of the Seismological Society of America. - 1974. - Vol. 64. - pp. 173-185.

Carafa P., Simonelli A. L. and Crewe A. J. Shaking table tests of gravity retaining walls to verify a displacement based design approach [Report]. - Rotterdam : 11th ECEE, 1998.

Cascone E. and Maugeri M. Shaking table tests of gravity reatining walls [Report]. - [s.l.] : Transaction on the built Environment vol 14, WIT Press, 1995.

Darendeli Mehmet Baris Development of a New Family of Normalized Modulus Reduction and Material Damping Curves [Report]. - [s.l.] : University of Texas at Austin, 2001.

EN1997-1 Eurocode 7: Geotechnical design - Part 1: General rules [Book]. - [s.l.] : approved by CEN, 2004.

EN1998-1 Eurocode 8: Design of structures for earthquake resistance - Part 1: General rules, seismic actions and rules for buildings [Book]. - [s.l.] : approved by CEN, 2004.

EN1998-5:1994 Eurocode 8: Design of structures for earthquake resistance. Part 5: Foundations, retaining structures and geotechnical aspects. [Book]. - [s.l.] : approved by CEN, 2004.

Fang Y. S., Yang Y. C. and Chen T. J. Retaining walls damaged in the Chi-Chi earthquake [Journal] // Can. Geotech. - 2003. - 40. - pp. 1142-1153.

Garini E., Gazetas G. and Anastasopoulos I. Asymmetric "Newmark" sliding caused by motions containing severe "directivity" and "fling" pulses [Journal] // Geotechnique. - 2011. - 61. - pp. 733-756.

Huang C. C., Wu S. H. and Wu H. J. Seismic Displacement Criterion for Soil Retaining Walls Based on Soil Strength Mobilization [Journal] // J. Geotech. Geoenviron. Eng.. - [s.l.] : ASCE, 2009. - 135. - pp. 74-83.

Ishihara Kenji Soil Behvaiour in Earthquake Geotechnics [Book]. - [s.l.] : Clarendon PRESS, Oxford, 1996.

Jibson Randall W. Predicting Earthquake-Induced Landslide Displacements Using Newmark's Sliding Block Analysis [Report]. - Washington, D.C. : Trasportation Research Board, National Research Council, 1993.
JRTRI Design guidline for railway structures-Aseismic design [Book]. - [s.l.] : Japanese Raylway Technical research Institute, 1999. - pp. 325-326.
Kramer Steven L. Geotechnical Earthquake Engineefing [Book]. - New Jersey : Prentice Hall, Inc, 1996.
Kulhawy F. H. and Mayne P. W. Manual on Estimating Soil Properties for Foundation Design [Report]. - [s.l.] : Electrical System Division, 1990.
Lo Grasso Agatino, Maugeri Michele and Motta Ernesto EXPERIMENTAL RESULTS ON EARTH PRESSURES ON RIGID WALL UNDER SEISMIC CONDITION [Report]. - Vancouver, Canada : 13WCEE, 2004.
Nadim F. and Whitman R. V. Seismically induced movement of retaining walls [Journal] // Journal of the Geotecnical Engineering Devision, ASCE. - 1983. - pp. 915-31.
Newmark N. Effects of erathquakes on dams and embankments [Journal] // Geotechnique. - 1965. - 2 : Vol. 15. - pp. 139-160.
Richard R. and Elms DG Seismic behaviour of gravity retaining walls. [Journal] // Journal of the Geotecnical Engineering Devision, ASCE . - 1979. - pp. 449-64.
Sarma S. K. Seismic stability of earth dams and embankments [Journal] // Geotechnique. - 1975. - pp. 743-761.
Simonelli Armando [et al.] Retainign Walls Under Seismic Actions: Shaking Table Testing and Numerical Approaches [Report]. - [s.l.] : 12WCEE, 2000.
Smith William K. Database of Newmark displacements, Arias intensities, and Dobry durations for selected horizontal-component stron-motion records. [Report] : Open-File Report 94-248 / U.S. Department of the Interior U.S. Geological Survey. - 1994.
Watanabe K. [et al.] Behaviour of several types of model reatining walls subjected to irregular excitation [Journal] // Soil and Foundation, Japanese Geotechnical Society. - [s.l.] : SOIL AND FOUNSATION Vol.43, , 2003. - pp. 13-27.
Whitman R. V. and Liao S. Seismic design of retaining walls [Report] : Miscellaneous Paper GL-85-l / U.S. Army Engineering Waterways Experiment Station. - Vicksburg, Mississippi : [s.n.], 1985.
Wilson R. C. and Keefer D. K. Predicting Areal Limits of Earthquake-iduced Landsliding. In Evaluating Earthquake Hazard in the Los Angeles Region - An Earth Science Perspective [Journal] // U.S. Geological Survey. - 1985. - pp. 316-345.
Wu Y. and Prakash S. On seismic displacements of rigid retaining walls [Journal] // Geotechnical Special Publication: Analysis and Design of Retainign Structures Against Earthquakes. - New York : ASCE, 1996. - pp. 21-37.
Zarrabi K. Sliding of gravity retaining wall during earthquakes considering vertical acceleration and changing inclination of failure surface [Report] / Department of Civil Engineering ; MIT. - Cambridge : SM Thesis, 1979.
Zhang Jian [et al.] Seismic damage of earth structures of road engineering in the 2008 Wenchuan earthquake [Journal] // Environ Earth Sci. - 2011. - 65. - pp. 987-993.